Analysis of membrane fouling by proteins during nanofiltration of chitin alkali wastewater

Juan Li, Liming Zhao, Yaosong Wang, Chaoqin Chen, Jiachun Zhou, Yongjun Qiu and Hailong Du

ABSTRACT

The membrane fouling mechanism used during the nanofiltration (NF) of chitin alkali effluent was investigated. Tests were carried out in three large-scale chitin-processing plants with three kinds of wastewater. An alkali resistant NF membrane with molecular weight cut-off of 250 Da was employed. The reflection coefficient (σ) and diffusion coefficient (P_s) of total proteins were deduced, assuming that the proteins were single entities in the feed. Viscosity and osmosis pressure were measured to evaluate their influences on the permeate flux. Furthermore, the fraction of the protein fouling was extracted and qualitatively analyzed by mass spectrometry. Results showed that the NF permeate flux of alkali wastewater with the highest protein concentration (4.00%) was the lowest, and that σ and penetration P_s decreased with protein content growth. Over 60% of the peptides in the permeate were hydrophobic, whereas 70% of the peptides in the adsorption cake were hydrophilic. Irreversible resistance was the predominant resistance during NF processing, and the fouling behaviour of hydrophilic fractions was dominant.

Key words | chitin alkali effluent, hydrophobic, protein fouling, nanofiltration

Juan Li
Liming Zhao (corresponding author)
Yaosong Wang
Chaoqin Chen
Jiachun Zhou
Yongjun Qiu
Hailong Du
State Key Laboratory of Bioreactor Engineering,
R&D Center of Separation and Extraction Technology in Fermentation Industry,
East China University of Science and Technology,
Shanghai 200237,
China
E-mail: *zhaoliming@ecust.edu.cn*

NOMENCLATURE

A_m	effect membrane area, m^2
C_F	crude protein concentration in the feed, Kg/Kg
C_P	crude protein concentration in the permeate, Kg/Kg
$J'_{v\cdot w}$	pure water permeate fluxes measured with the fouling nanofiltration membrane (NFM) after the equipment is flushed with deionized (DI) water up to pH 7.0, $L\,m^{-2}\,h^{-1}$
J_v	permeate flux, $L\,m^{-2}\,h^{-1}$
$J_{v\cdot w}$	pure water permeate fluxes measured with the virgin NFM, $L\,m^{-2}\,h^{-1}$
P_{in}	pressures procured at the inlet of the membrane, bar
P_{out}	pressures procured at the outlet of the membrane, bar
P_s	penetration coefficient of the solute, $L\,m^{-2}h^{-1}$
R	rejection of protein hydrolysates, dimensionless
R'_m	contaminative membrane resistance, m^{-1}
R_f	membrane fouling resistance, m^{-1}
R_{irr}	irreversible fouling resistance, m^{-1}
R_m	membrane inherent resistance, m^{-1}
R_r	reversible fouling resistance, m^{-1}
TMP	transmembrane pressure, bar
V_p	permeate volume during the measured time, L

Greek letters

Δt	time of the flow, h
$\Delta\Pi$	osmotic pressure difference between both sides of membrane, bar
η_w	dynamic viscosities of DI water, bar · h
σ	rejection coefficient of the membrane towards a solute, dimensionless

Subscripts

F	feed
f	fouling
in	inlet

doi: 10.2166/wrd.2014.005

irr irreversible
m membrane
out outlet
P permeate
r reversible
v volume
w water

INTRODUCTION

Nanofiltration (NF) is an effective and reliable method for the combined removal of a broad range of pollutants in surface water and effluent discharged from the food, industry and dye industries. However, one of the main obstacles to NF technology application is membrane fouling. Fouling in general causes deterioration in permeate quality and quantity, i.e. the ratio of permeate to feed stream, to values of about 80% in the drinking water industry (Nederlof *et al.* 2005), and eventually membrane replacement is unavoidable (Listiarini *et al.* 2009). In normal operation, fouling manifests itself as flux decline and decreased transmission over time, resulting from reversible accumulation of solutes at the membrane surface, more commonly known as 'concentration polarization (CP)', progressing to irreversible adsorption and cake build-up.

For deproteination processing in chitin production, approximately 4% (w/w) of NaOH is used at about 10–15 times concentration of shrimp discards (w/v). The alkali wastewater discharged from chitin processing is abundant in protein hydrolysates which can be separated and concentrated selectively by an alkali-tolerant nanofiltration membrane (NFM) (Tsuru *et al.* 1994; Gésan-Guiziou *et al.* 2007; Zhao & Xia 2009). The recovery of NaOH and protein hydrolytes could be essentially significant from both an ecological and economic point of view. However, the membrane fouling by proteins and their hydrolysates during the NF of chitin alkali effluents is far from certain, which plays an important role in the application of NF.

As the feed is abundant in proteins, especially in the case of chitin alkali wastewater, the principal membrane fouling is usually attributed to interaction between proteins and the membrane. Characterization of protein-fouling membranes is crucial to understanding the fouling mechanisms, for the optimization of fouling control and for the cleaning method. Like other types of solutes, fouling by proteins and their hydrolysates has traditionally been characterized via the monitoring of flux decline and observation of rejection changes. Some techniques, such as scanning electron microscopy and energy dispersive X-ray spectroscopy, have particularly highlighted the change in foulant morphology from cake to aggregate formation as a function of flux and membrane morphology. Improvement in fixation technique, staining and coating have reduced artifacts and even removed the need for a vacuum with the advent of the environmental scanning electron microscope (Baumgarten 1990). However, internal deposition with pore blocking at low foulant levels remains difficult to detect.

This study focused on the NF process characteristics of three kinds of chitin alkali effluents made up of portunid, *Chionoecetes bairdi* and *Eriocheir sinensis* carapaces, respectively, in three typical large-scale chitin-processing plants. Ultrafiltration as a pretreatment of the effluent was operated by a stainless steel membrane prior to NF, and detailed analysis of proteins fouling on the membrane during NF was conducted in this study.

MATERIALS AND METHODS

Materials and chemicals

The alkali wastewaters coming from different raw materials, i.e. *Chionoecetes bairdi* chitin (CBCAW), portunid chitin (PCAW) and *Eriocheir sinensis* chitin (ESCAW), discharged from chitin-processing, were supplied by Qingdao Yunzhou Biotech Co. Ltd (Qingdao, China), Jiangshu Shuanglin Biotech Co. Ltd (Nantong, China) and Rixing Biotech Co. Ltd (Yangzhou, China), respectively.

Concentrated sulfuric acid, boracic acid, cupric sulfate, potassium sulfate, sodium hydroxide, hydrochloric acid, ethylene diamine tetraacetic acid (EDTA) and barium hydroxide were purchased from China National Medicine Co. Ltd (Shanghai, China). Trifluoroacetic acid (TFA) and alpha-

cyano-4-hydroxycin-namic acid (CHCA) were obtained from Sigma Chemical Co. (St Louis, MO, USA). All reagents were of analytical grade.

Membrane modules

Stainless steel microfiltration (SSM) in a tube configuration was supplied by Hydrochem Ltd (Hyflux, Singapore). The alkali-tolerant NFM in spiral-wound configuration was purchased from Koch Co. (USA). The pilot setup was supplied by Shanghai Qiyu Biotech. Ltd. Specifications of each module are summarized in Table 1.

Analysis of effluent

For the identical alkali effluents, the main components were analyzed in our previous work, and the total crude proteins are the primary component in the alkali effluent (Zhao *et al.* 2013). To explore the influence of the viscosity and osmosis pressure of the alkali effluent on the decline of permeate flux, the two parameters were measured. The viscosity of the effluent was measured at 40 °C (Butylina *et al.* 2006) and the osmotic pressure of the effluent was determined with a freezing point osmometer (Vilker *et al.* 1981).

Experimental protocol for NF

NF full circulation of three effluents and Matlab analog

Prior to the NF of the alkali effluents, the ultrafiltration of the effluents by SSM was carried out to remove insoluble substances. The operation of the SSM module was fixed at 80 ± 1 °C and a transmembrane pressure (TMP) of 3.1 bar (Zhao & Xia 2009). The permeate from the SSM (SSM-P) module was pumped into the feed tank of the NF set-up and the retentate was recycled back to the feed tank of the SSM set-up. Upon the 30 L of SSM-P cooling down to 40 ± 1 °C, the NF was run at full-circulation mode at different TMP. After each TMP up to stabilization, before setting another pressure,

Table 1 | Specific parameters of the membrane modules

Module	SSM[a] module (L-400)	NF[b] module (MPS-34 2540 A2X)
Membrane area (m^2)	0.35	1.6
MWCO[c] (g/mol)	50,000	200 (initial)
Module length (m)	1.50	1.02
Equipment version	L-400	M104-3
Membrane material	316 L Stainless + TiO_2	Proprietary composite NFM[d]
Tube material	304 Stainless steel	304 Stainless steel
P_{max} (bar)	60	35
T_{max} (°C)	177	50
Construction	Tubular wound	Spiral wound
Nominal solute rejections (%)	–[e]	95 Glucose/35 NaCl
Feed spacer (mm)	–[e]	0.8
Allowable pH-continuous operation	2–14[f]	1–14[f]
Allowable pH-clean-in-place (CIP)	2–14[f]	1–14[f]

[a]SSM refers to stainless steel microfiltration.
[b]NF refers to nanofiltration.
[c]MWCO refers to molecular weight cut-off.
[d]NFM is made of chlorinated polyvinyl chloride.
[e]'–' represents permeated.
[f]Avoid corrosive acid when using a stainless steel permeate tube.

permeate flux was essentially measured according to Equation (1):

$$J_v = V_p/(A_m \cdot \Delta t) \quad (1)$$

where J_v is permeate flux, V_p is permeate volume during the measured time, A_m is effect membrane area, and Δt is time of the flow. The sample was taken for calculating total rejection of crude proteins on the basis of Equation (2):

$$R = 1 - C_p/C_F \quad (2)$$

where R is rejection of the protein hydrolysates, and C_F and C_P are crude proteins concentrations in the feed and in the permeate, respectively.

Based on the Spiegler–Kedem (S–K) formula (Equation (3)), the relationship between permeates fluxes and rejections of crude proteins were simulated by Matlab, which was beneficial for deducing the reflection coefficient (σ) and diffusion coefficient (P_s) of crude proteins according to Equation (3):

$$R = 1 - (1 - \sigma)/(1 - \delta \cdot \exp(1 - J_v \cdot (1 - \sigma)/P_S)) \quad (3)$$

where R is real rejections, non-dimensional, J_v is permeate flux, σ is the rejection coefficient of the membrane towards a particular solute, and P_s is the penetration coefficient of the solute. Under normal conditions, the S-K formula is applied to analog the NF characteristic parameters of the pure materials. However, as the total crude proteins and their hydrolysates are the main components in the effluents, it is feasible to assume that the crude proteins are a single component during the study to avoid complicated calculation.

NF concentration of effluent

NF was run at the maximum TMP (usually 35 bar below) that the NF equipment and NFM could withstand. Specifically, the SSM-P was continuously pumped into the feed tank of the NF set-up to maintain constant volume, preventing the density of the feed from instant growing. The back-flow velocity was set at 2.7 m/s (Gésan-Guiziou *et al.* 2007) to force the fluid surrounding the membrane surface to flow in turbulence, which could resist the tendency to CP and membrane fouling. The NF retentate returned to the NF feed tank while the NF permeate (NF-P) was collected in containers. The permeate fluxes were measured in every 2 L of permeate and calculated according to Equation (1). Samples of permeate and retentate were taken every hour for analysis. When the flux declined to approximately 5.0 L/(m^2 h) (LMH), the NF of the effluent was terminated.

Loss ratio of DI water permeate flux

Prior to measuring the NF concentration of each batch effluent, DI water permeate flux was measured with the virgin NF membrane (NFM). After finishing the NF concentration of each effluent, the NF module was flushed with DI water until the pH of feedback water was 7, which ensured that the effluent in the dead volume was completely removed from the NF system, and then DI water permeate fluxes were measured with the fouled NFM relevant to CBCAW, PCAW and ESCAW, respectively. The loss ratio of the DI water permeate flux was calculated in accordance with Equation (4):

$$L_{\text{flux}} = (1 - J'_{v\cdot w}/J_{v\cdot w}) \times 100\% \quad (4)$$

where L_{flux} is loss of permeate flux, $J_{v\cdot w}$ is permeate flux of DI water measured with the virgin membrane, and $J'_{v\cdot w}$ is permeate flux of DI water measured with the fouled membrane.

Relevant resistance deduced

The pure water flux of the virgin NF membrane was measured (at 30 °C, 17 bar) prior to the NF-concentration of the effluent, and that of the foul membrane was measured when the membrane was flushed to pH 7 with the DI water after the NF concentration of the wastewater. The procedure as stated above aimed to determine the relevant membrane resistances. The membrane inherent resistance could be calculated by Equations (5) and (6). Referring to Equations (7) and (8), the irreversible membrane fouling resistance (R_{irr}) could be deduced. Afterwards, the total membrane fouling resistance (R_f) could be deduced from Equation (9). Finally, the reversible membrane fouling resistance (R_r) could be acquired according to Equation (10).

$$\text{TMP} = \frac{P_{\text{in}} + P_{\text{out}}}{2} - P_p \quad (5)$$

where TMP is transmembrane pressure, P_p is pressure obtained after the transmitted membrane and usually

omitted, P_{in} and P_{out} are pressures procured at the inlet and at the outlet of the membrane, respectively.

$$J_{v\cdot w} = \frac{\mathrm{TMP}}{\eta_w \cdot R_m} \tag{6}$$

$$J'_{v\cdot w} = \frac{\mathrm{TMP}}{\eta_w \cdot R'_m} \tag{7}$$

$$R'_m = R_m + R_{\mathrm{irr}} \tag{8}$$

$$J_v = \frac{\mathrm{d}V_p}{A_m \cdot \mathrm{d}t} = \frac{\mathrm{TMP} - \sigma \cdot \Delta\prod}{\eta_s \cdot (R_m + R_f)} \tag{9}$$

$$R_f = R_r + R_{\mathrm{irr}} \tag{10}$$

where $J_{v\cdot w}$ and $J'_{v\cdot w}$ are the pure water permeate fluxes measured with the virgin NF membrane with the fouling NF membrane after the equipment was flushed with DI water up to pH 7, respectively; η_w and η_s are dynamic viscosities of DI water and permeate solution, respectively; R_m, R'_m, R_f, R_{irr}, and R_r are membrane inherent resistance, contaminative membrane resistance, membrane fouling resistance, irreversible fouling resistance and reversible fouling resistance, respectively; σ is the rejection coefficient of the membrane towards a particular solute, and $\Delta\Pi$ is the osmotic pressure difference across the membrane.

Fraction of protein-hydrolysates adsorbing NFM

The NF system was then cleaned according to the following procedures specified by the manufacture and flushed with an adequate amount of DI water between each step: (1) full recirculation cycle with 1.5% (w/v) NaOH consisting of 0.05% (w/w) EDTA at TMP of 5 bar and 50 °C for 30 min; (2) full recirculation cycle with 0.5% (v/v) HNO_3 at TMP of 5 bar and 50 °C for 40 min; and (3) full recirculation cycle with 1.5% (w/v) NaOH consisting of 0.05% (w/w) EDTA at TMP of 5 bar and 50 °C for 30 min. Finally, to extract the fraction of protein-hydrolysates adsorbed on the NFM, the alkali lotion procured from the two alkali flushing procedures was merged into the acid lotion obtained from the acid flushing procedure.

Characterization of protein-hydrolysates adsorbed on the NFM

Sample preparation

Because of the fraction of protein-hydrolysates adsorbed on the NFM containing inorganic compounds, it was essential to desalt the sample by a Strata™ solid phase extraction column (Phenomenex, Torrance, CA, USA) prior to matrix-assisted laser desorption/ionization time-of-flight/time-of-flight tandem mass spectrometry (MALDI-TOF/TOF-MS/MS) analysis to ensure high accuracy. CHCA as the matrix was used at a concentration of 10 mg/mL and resuspended in a 1:1 mixture (v/v) of acetonitrile and 0.1% TFA/water. Finally, the resulting mixture (1 μL) was deposited on the MALDI-TOF sample holder.

Peptides identified by MALDI-TOF/TOF-MS/MS

Mass spectrometry followed the main procedure, as described by Cucu *et al.* (2012). A 4800 plus MALDI-TOF/TOF MS Analyzer (AB Sciex, Foster City, USA) equipped with an Nd:YAG laser emitting at 355 nm was employed to perform data acquisition in a positive-ion mode reflectron for peptide detection. The acceleration voltage was set at 20 kV and the extraction delay time used was 450 ns in reflector MS mode. Using calibration peptides, the amount of the peptides was determined. MS and MS/MS data were processed using a 4000 Series Explorer and further manually interpreted using DATA Explorer 4.8 (AB Sciex, USA) software. In MS mode, 400 shots were accumulated and in MS/MS mode 1,000 shots were accumulated for the peptides with high intensity. An amino acid sequence was performed on a DeNovo Explorer™ (AB Sciex, USA). The amino acid sequence was confirmed by manual validation.

RESULTS AND DISCUSSION

Physical characteristic analysis of the alkali effluent

The contents of the different compounds in the three alkali wastewaters and their pH and viscosities are listed in Table 2, implying that crude proteins were the predominant

Table 2 | Component analysis of three alkali effluents

Composition	PCAW		CBCAW		ESCAW	
	Content in the crude (%)	Content in the SSM-P (%)	Content in the crude (%)	Content in the SSM-P (%)	Content in the crude (%)	Content in the SSM-P (%)
Dry matter	6.52	5.6	3.47	3.2629	8.5	7.13
Ash	4.44	3.97	2.42	2.3	3.35	2.68
Protein	1.81	1.57	0.70	0.78	5.25	4.20
Lipid	0.11	0.03	0.28	0.05	0.32	0.04
Saccharide	0.09	0.02	0.12	0.0688	0.07	0.04
NaOH	2.83	2.19	1.36	1.34	0.83	0.67
pH	14	14	14	14	14	14
Viscosity(μPa S)	ND[a]	680	ND[a]	670.253	ND[a]	860

[a]ND (not detected) because of suspended solids.

components in the three chitin alkali effluents, which was similar to our previous study (Zhao *et al.* 2013). It was also found that both the viscosity and osmosis pressure of the chitin alkali effluents were proportional to crude protein concentration (Figure 1). Within protein concentrations ranging from 0.7 to 4.2% (W/W), the viscosities of the stainless steel microfiltration permeate (SSM-P) ranged from 680 to 860 bar h, and the osmosis pressure differences ($\Delta\Pi$) between NF feed (NF-F) and NF permeate (NF-P) were in the range of 4 to 18 bar. Given that the total protein concentration (4.2%) of ESCAW was much bigger than those of CBCAW (1.57%) and PCAW (0.7%), the NF net drive forces of the three chitin alkali effluents decreased in the order of PCAW, CBCAW, ESCAW, which complied with the K-K formula (Jarzyńska & Pietruszka 2011).

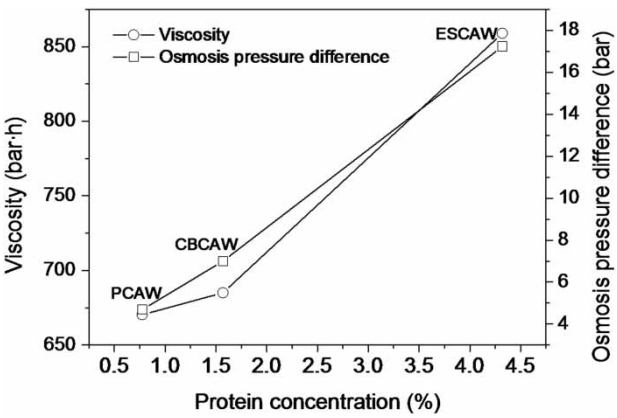

Figure 1 | Viscosity of the permeate and osmosis pressure difference between the permeate and the feed versus the concentration of crude protein in the alkali wastewater.

Characteristic parameters of NF of the effluent

As seen from Figure 2(a), rejections of crude proteins are proportional to the permeate fluxes of chitin alkali effluent, complying with the S-K formula despite the chitin alkali wastewater being a complicated mixture. Furthermore, permeate fluxes relevant to the NF of ESCAW are substantially lower than those related to the NF of CBCAW, which are much lower than those relevant to the NF of PCAW chitin alkali effluent (Figure 1), which is mainly because the NF net drive forces of the three chitin alkali effluents decreased in the order of PCAW, CBCAW and ESCAW (as presented in Figure 1).

Otherwise, both σ and P_s decrease with the crude protein concentrations, as implied in Figure 2(b). Theoretically, σ is approximately equal to the rejection of total proteins when permeate fluxes are infinitely great, and the rejections of total proteins and their concentrations had an inverse relationship (Catarino & Minhalma 2008; Curcio & Drioli 2009; Feng *et al.* 2009). Therefore, it was reasonable that σ of total proteins was an inverse ratio to their concentration. On the basis of Equation (5), for the identical solution, P_s of the solute is inversely proportional to the density and viscosity of the solution, both of which

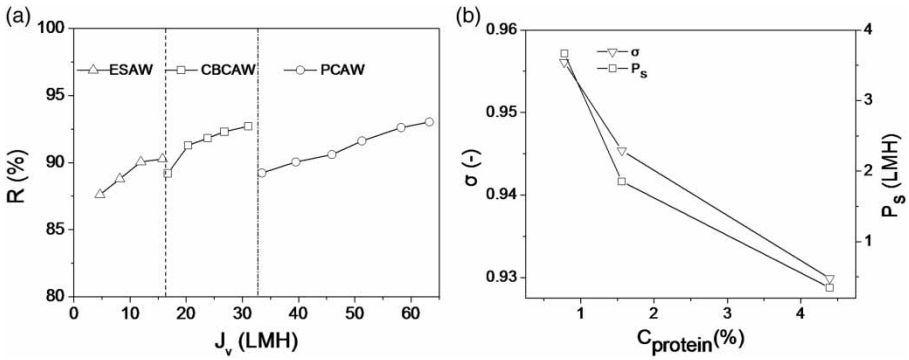

Figure 2 | The relationship between total protein rejections and permeate fluxes for three chitin alkali effluents (a), and reflection coefficient (δ) and permeate coefficient (P_s) of total protein versus protein contents (b).

increase with solute concentration (Jarzyńska & Pietruszka 2011). As a consequence, P_s of total proteins decreased with their content's growth.

$$P_s = P_{sw} \cdot (\eta_w \rho_w / \eta \rho) \tag{11}$$

Permeate flux and resistance

Figure 3(a) shows that there is a steady decline in the permeate fluxes of the three chitin alkali wastewaters over permeate time growing. At the first stage of NF, permeate flux of the NF of PCAW is higher than that of CBCAW, which is higher than that of the NF of ESCAW, because the total protein concentration in PCAW is much lower than that in ESCAW followed by that in CBCAW. Both osmosis pressure and viscosity of the wastewater are proportional to the crude protein contents in the alkali effluents (Figure 1). As known, osmosis pressure usually lowers the net driven force and permeate flux is reverse proportional to the viscosity of the permeate. Therefore, it is reasonable that the difference among permeate fluxes is relevant to the three effluents. As illustrated in Figure 3(b), the resistance generated from the filtration cake (R_c) to the total resistance (R_f) ratios (R_c/R_f) increases over permeate time during NF. It is also implied that the R_c/R_f relevant to the NF of CBCAW is the smallest one of the three ratios. Additionally, the loss of DI water permeate flux for CBCAW was the highest among the three alkali effluents (Figure 4). Therefore, it could be concluded that the ratio of irreversible resistance in the NF of CBCAW to the total resistance was much larger than those in the NF of PCAW and ESCAW.

Further, the irreversible adsorption and pore blocking also play an important role in the membrane resistance, and the results obtained in a previous work show that the total R_{irr} formed by pore constriction to the total foul resistance R_f was up to 14.06% (Zhao *et al.* 2013).

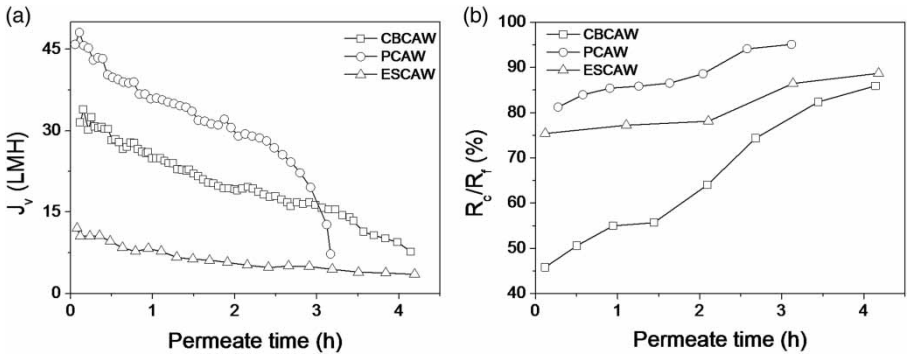

Figure 3 | Permeate fluxes of three chitin alkali wastewaters (a) and R_c/R_f during NF of three chitin alkali wastewaters versus permeate time (b). R_c and R_f mean resistance generated from the filtration cake and membrane fouling resistance, respectively.

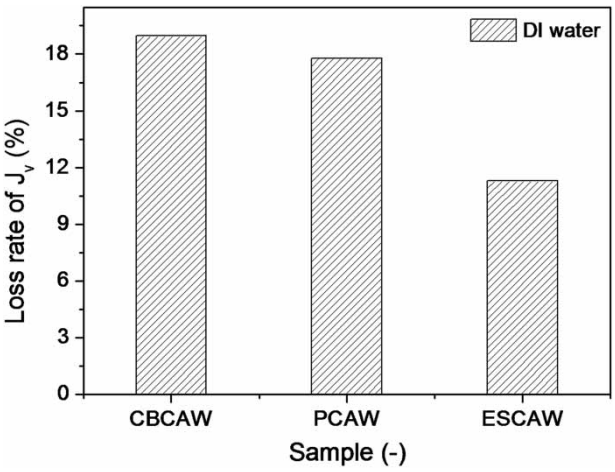

Figure 4 | Loss rates of DI water measured with the fouled NFM procured from NF of three chitin alkali wastewaters (CBCAW, PCAW and ESCAW). CBCAW, PCAW and ESCAW are *Chionoecetes bairdi* chitin alkali wastewater, portunid chitin alkali wastewater and *Eriocheir sinensis* alkali wastewater, respectively.

Analysis of protein fouling

A conclusion was drawn that the irreversible resistance produced from NF of CBCAW is much larger than those generated by the other two effluents. Hence, a mass spectrum (MS) analysis of the fraction of protein-hydrolysates adsorbed on the NFM was introduced to investigate the fouling mechanism underlying NF of CBCAW.

Tables 2–4 present the amino acid sequences, molecular weight (MW) and isoelectric points (pI) of the representative peptides in the feed, permeate and the adsorption of CBCAW. It could be concluded that the rejection of some peptides (KNSTP, FIPTSMHG, PEHAPVGID, FPLEYKTKVA, EDLYSTPKLEEL) in the NF-adsorption was mainly because of the higher MW than those in NF-P (Tables 4 and 5). In terms of the peptides' GRAVY (grand average of hydropathy), 60% of the peptides in the permeate

Table 3 | Main biochemistry characteristics of the representative peptides in NF-F

Amino acid sequence	MW[a]/(g/mol)	pI[a]	GRAVY[a]
PAL	300.3	5.96	1.33
LGL	302.3	5.52	1.37
DGL	304.3	3.8	− 0.03
SLS	306.2	5.24	0.73
PVV	314.2	5.96	2.27
VESC	437.3	4	0.60
ESLT	449.3	4	− 1.20
LGMAT	492.3	5.52	1.28
KNSTP	546.4	8.75	− 2.10
FAKNTPS	764.5	8.75	− 0.84
AGGPGGSAVT	773.5	5.57	0.31
GGAGRGAAYG	836.5	8.75	− 0.24
KIPTSMHG	870.6	8.76	− 0.53
PEHAPVGID	934.6	4.35	− 3.67
TVLRGDKY	951.5	8.25	− 0.79
FPLEYKTKVA	1195.7	8.5	− 0.23
CELCSAYYANK	1264.7	5.99	− 0.17
GARASAHNAPRDGI	1392.8	9.61	0.76
CWWGVGPFVFTSC	1488.8	5.51	1.02
YPFWDLETDPCL	1498.8	3.49	− 0.31

[a]pI, MW and GRAVY were calculated by an ExPASy Molecular Biology Server.

Table 4 | Main biochemistry characteristics of the representative peptides in NF-P

Amino acid sequence	MW[a] (g/mol)	pI[a]	GRAVY[a]
PAL	300.3	5.96	1.33
LGL	302.3	5.52	1.37
SLS	306.2	5.24	0.73
PVV	314.2	5.96	2.27
SPL	316.3	5.24	0.47
SVL	318.3	5.24	2.40
TPL	330.3	5.19	0.50
CPL	332.3	5.52	1.57
MPS	334.3	5.28	− 0.17
VLL	344.3	5.49	3.93
LLT	346.3	5.52	2.30
THV	356.3	6.40	0.10
THV	356.3	6.40	0.10
KKS	362.3	10.00	− 2.87
GGKL	374.3	8.75	− 0.30
KMT	379.1	8.75	− 0.90
KAAT	390.3	8.75	− 0.25
KKM	406.3	10.00	− 1.97
KGMD	450.4	5.84	− 1.48
CKPM	478.3	8.22	− 0.28

[a]pI, MW and GRAVY were calculated by an ExPASy Molecular Biology Server.

Table 5 | Main characteristics of peptides in the adsorption of NFM

Amino acid sequence	MW[a] (g/mol)	pI[a]	GRAVY[a]
PAL	300.2	5.96	1.33
DGL	304.3	3.80	– 0.03
SPL	316.3	5.24	0.47
SVL	318.2	5.24	2.40
TDT	336.2	3.80	– 1.63
VLL	344.3	5.49	3.93
LLT	346.3	5.52	2.30
LDT	348.2	3.80	– 0.13
HPP	350.2	6.74	– 2.13
KKS	362.3	10.00	– 2.87
KGGC	364.2	8.22	– 0.55
KAAT	388.3	8.75	– 0.25
KVF	393.3	8.75	1.03
DTAH	443.2	5.08	– 1.40
ESLT	449.3	4.00	– 1.20
KNSTP	546.3	8.75	– 2.10
KIPTSMHG	870.5	8.76	– 0.53
PEHAPVGID	934.5	4.35	– 3.67
FPLEYKTKVA	1195.6	8.50	– 0.23
EDLYSTPKLEEL	1436.8	4.00	– 0.91

[a]pI, MW and GRAVY were calculated by an ExPASy Molecular Biology Server.

have a GRAVY greater than 0, whereas 70% of the peptides in the foulant cake have a GRAVY less than 0. In other words, most peptides in the permeate are hydrophobic while most peptides in the foulant are hydrophilic. Therefore, it could be indicated that the fouling behaviour of the hydrophilic fractions was dominant. It has also been suggested (Kimura *et al.* 2006; Zularisam *et al.* 2007) that relatively hydrophilic natural organic matter source water exhibits a greater flux decline than does hydrophobic.

CONCLUSION

The NF membrane fouling mechanism of chitin processing alkali effluents was studied. Results indicate that σ and P_s were reversely proportional to protein concentrations, and the permeate flux of a high protein concentration feed was the lowest. In comparison with permeate flux loss and R_c/R_f, it could be speculated that severe protein fouling on the membrane surface occurred during NF of CBCAW. Therefore, complete identification of the peptides was realized by MALDI-TOF-MS. Most of the peptides in the permeate were hydrophobic whereas most peptides in the foulant were hydrophilic, indicating that the fouling behaviour of hydrophilic fractions was dominant.

ACKNOWLEDGEMENTS

This work was financially supported by the National Natural Science Foundation of China (grant no. 31101381) and also by the Fundamental Research Funds for the Central Universities (NO.WF1214060).

REFERENCES

Baumgarten, N. 1990 SEM for imaging specimens in their natural state. *Am. Lab.* **22**, 66.

Butylina, S., Luque, S. & Nyström, M. 2006 Fractionation of whey-derived peptides using a combination of ultrafiltration and nanofiltration. *J. Membr. Sci.* **280**, 418–426.

Catarino, I. & Minhalma, M. 2008 Assessment of saccharide fractionation by ultrafiltration and nanofiltration. *J. Membr. Sci.* **312**, 34–40.

Cucu, T., Meulenaer, B. D., Kerkaert, B., Vandenberghe, I. & Devreese, B. 2012 MALDI based identification of whey protein derived tryptic marker peptides that resist protein glycation. *Food Res. Int.* **47**, 23–30.

Curcio, E. & Drioli, E. 2009 *Membranes for Desalination. Seawater Desalination*. Springer, Berlin Heidelberg, pp. 41–75.

Feng, Y. M., Chang, X. L., Wang, W. H. & Ma, R. Y. 2009 Separation of galacto-oligosaccharides mixture by nanofiltration. *J. Taiwan. Inst. Chem. Eng.* **40**, 326–332.

Gésan-Guiziou, G., Alvarez, N., Jacob, D. & Daufin, G. 2007 Cleaning-in-place coupled with membrane regeneration for re-using caustic soda solutions. *Sep. Purif. Technol.* **54**, 329–339.

Jarzyńska, M. & Pietruszka, M. 2011 The application of the Kedem–Katchalsky equations to membrane transport of ethyl alcohol and glucose. *Desalination* **280**, 14–19.

Kimura, K., Yamamura, H. & Watanabe, Y. 2006 Irreversible fouling in MF/UF membranes caused by natural organic matters (NOMs) isolated from different origins. *Sep. Sci. Technol.* **41**, 1331–1344.

Listiarini, K., Chun, W., Sun, D. D. & Leckie, J. O. 2009 Fouling mechanism and resistance analyses of systems containing

sodium alginate, calcium, alum and their combination in dead-end fouling of nanofiltration membranes. *J. Membr. Sci.* **344**, 244–251.

Nederlof, M. M., Paassen, J. A. M. V. & Jong, R. 2005 Nanofiltration concentrate disposal:experiences in the Netherlands. *Desalination* **178**, 303–312.

Tsuru, T., Shutou, T., Nakao, S. I. & Kimura, S. 1994 Peptide and amino acid separation with nanofiltration membranes. *Sep. Purif. Technol.* **29**, 971–984.

Vilker, V. L., Colton, C. K. & Smith, K. A. 1981 The osmotic pressure of concentrated protein solutions: Effect of concentration and ph in saline solutions of bovine serum albumin. *J. Colloid Interface Sci.* **79**, 548–566.

Zhao, L. M. & Xia, W. S. 2009 Stainless steel membrane UF coupled with NF process for the recovery of sodium hydroxide from alkaline wastewater in chitin processing. *Desalination* **249**, 774–780.

Zhao, L., Li, J., Wang, Y., Fan, J. & Li, A. 2013 Mechanism underlying the nanofiltration of protein hydrolysates in chitin alkali wastewater. *Desalin. Water Treat.* doi: 10.1080/19443994.2013.823356.

Zularisam, A. W., Ismail, A. F., Salim, M. R., Sakinah, M. & Hiroaki, O. 2007 Fabrication, fouling and foulant analyses of asymmetric polysulfone (PSF) ultrafiltration membrane fouled with natural organic matter (NOM) source waters. *J. Membr. Sci.* **299**, 97–113.

First received 20 January 2014; accepted in revised form 28 March 2014. Available online 22 April 2014